

Efficient dynamic events discrimination technique for fiber distributed Brillouin sensors

Carlos A. Galindez,* Francisco J. Madruga, and Jose M. Lopez-Higuera

Photonics Engineering Group, Universidad de Cantabria, Edif. I + D + i de Telecomunicaciones, Avda. Castros s/n,
39005 Santander, Spain

*galindezca@unican.es

Abstract: A technique to detect real time variations of temperature or strain in Brillouin based distributed fiber sensors is proposed and is investigated in this paper. The technique is based on anomaly detection methods such as the RX-algorithm. Detection and isolation of dynamic events from the static ones are demonstrated by a proper processing of the Brillouin gain values obtained by using a standard BOTDA system. Results also suggest that better signal to noise ratio, dynamic range and spatial resolution can be obtained. For a pump pulse of 5 ns the spatial resolution is enhanced, (from 0.541 m obtained by direct gain measurement, to 0.418 m obtained with the technique here exposed) since the analysis is concentrated in the variation of the Brillouin gain and not only on the averaging of the signal along the time.

© 2011 Optical Society of America

OCIS codes: (060.2370) Fiber optics sensors; (190.4370) Nonlinear optics, fibers; (290.5900) Scattering, stimulated Brillouin.

References and links

1. C. Galindez and J. M. Lopez-Higuera, "Decimeter spatial resolution by using differential pre-excitation BOTDA pulse technique," *IEEE Sens. J.* **PP**(99), 1–1 (2011).
 2. A. Minardo, R. Bernini, and L. Zeni, "Stimulated Brillouin scattering modeling for high-resolution, time-domain distributed sensing," *Opt. Express* **15**(16), 10397–10407 (2007).
 3. K. Y. Song, Z. He, and K. Hotate, "Distributed strain measurement with millimeter-order spatial resolution based on Brillouin optical correlation domain analysis," *Opt. Lett.* **31**(17), 2526–2528 (2006).
 4. M. A. Soto, G. Bolognini, and F. Di Pasquale, "Long-range simplex-coded BOTDA sensor over 120 km distance employing optical preamplification," *Opt. Lett.* **36**(2), 232–234 (2011).
 5. A. Zornoza, A. Minardo, R. Bernini, A. Loayssa, and L. Zeni, "Pulsing the probe wave to reduce nonlocal effects in Brillouin optical time-domain analysis sensors," *IEEE Sens. J.* **11**, 1067–1068 (2011).
 6. T. Horiguchi, T. Kurashima, and M. Tateda, "Technique to measure distributed strain in optical fibers," *IEEE Photon. Technol. Lett.* **2**(5), 352–354 (1990).
 7. T. Kurashima, T. Horiguchi, and M. Tateda, "Distributed-temperature sensing using stimulated Brillouin scattering in optical silica fibers," *Opt. Lett.* **15**(18), 1038–1040 (1990).
 8. Z. Liu, G. Ferrier, X. Bao, X. Zeng, Q. Yu, and A. Kim, "Brillouin Scattering Based Distributed Fiber Optic Temperature Sensing for Fire Detection," in *Proceedings of The 7th International Symposium on Fire Safety Conference (Worcester, 2002)*.
 9. R. Bernini, A. Minardo, and L. Zeni, "Dynamic strain measurement in optical fibers by stimulated Brillouin scattering," *Opt. Lett.* **34**(17), 2613–2615 (2009).
 10. X. Bao, C. Zhang, W. Li, M. Eisa, S. El-Gamal, and B. Benmokrane, "Monitoring the distributed impact wave on a concrete slab due to the traffic based on polarization dependence on stimulated Brillouin scattering," *Smart Mater. Struct.* **17**(1), 015003 (2008).
 11. P. Chaube, B. G. Colpitts, D. Jagannathan, and A. W. Brown, "Distributed Fiber-Optic Sensor for Dynamic Strain Measurement," *IEEE Sens. J.* **8**(7), 1067–1072 (2008).
 12. K. Y. Song and K. Hotate, "Distributed Fiber Strain Sensor With 1-kHz Sampling Rate Based on Brillouin Optical Correlation Domain Analysis," *IEEE Photon. Technol. Lett.* **19**(23), 1928–1930 (2007).
 13. R. W. Boyd, *Non linear Optics* (Academic Press; Elsevier Science, 2003).
 14. C. Galindez, F. J. Madruga, and J. M. Lopez-Higuera, "Brillouin frequency shift of standard optical fibers set in water vapor medium," *Opt. Lett.* **35**(1), 28–30 (2010).
 15. I. S. Reed and X. Yu, "Adaptive multiple-band CFAR detection of an optical pattern with unknown spectral distribution," *IEEE Trans. Acoust. Speech Signal Process.* **38**(10), 1760–1770 (1990).
-

1. Introduction

Distributed Brillouin fiber sensors are very attractive for a wide set of applications (including health structural monitoring), since they can provide centimeter resolutions [1–3], measurement ranges of kilometers [4,5] and high sensitivity to the temperature and deformations experienced by the sensing fiber [6,7]. Stimulated Brillouin scattering (SBS) based on fiber optic sensors use the phase matching between the pump and the Stokes counter-propagating optical waves and an acoustic wave. Such interaction is maximized for a precise value of frequency shift between the two optical waves, which is strongly dependent of the temperature and strain into the material.

In fiber distributed sensors the information of the temperature or the strain can be located by a pulsed optical wave such is the case of the Brillouin optical time domain analysis (BOTDA) or by Brillouin optical frequency correlation domain analysis (BOCDA) techniques. Nevertheless, the measurement time required by a traditional BOTDA system is on the order of minutes, time that also depends on the total length range and constitutes a serious drawback for dynamic detection.

Dynamic variations of temperature or strain can be measured using SBS sensors by modifying the sensor technique or system. The simplest method consists on the directly measurement of the intensity of the Brillouin peak gain/loss signal versus time, allowing the use of a BOTDA system [8], which drastically reduces the measurement time, but it has a threshold detection and requires high averaging sampling as the length range is enlarged. Similar to this idea is the technique that uses two counter-propagating optical pulses with a fixed optical frequency difference; this difference is set to a spectral distance from the local Brillouin frequency shift approximately equal to half the Brillouin gain spectrum linewidth; then any vibration-induced modulation of the local Brillouin frequency shift will be measured as an intensity variation of the Stokes pulse peak intensity [9]. Important changes in the setup are required in this technique and non-periodic dynamic variations are not detected. There are other methods, e.g. one that uses the polarization dependence of the Brillouin gain to avoid the need for scanning the pump–probe frequency shift [10]. To reduce the measurement time, a technique based on a multitude of pump signals in the form of a frequency-domain comb in a complex BOTDA based system is also proposed [11]. A different attempt to enhance the Brillouin technique is a correlation-based cw technique; it is capable of making distributed dynamic strain measurements of vibrations up to 200 Hz with 10 cm spatial resolution [12]. However, this correlation technique has some limitations in terms of maximum sensing length and setup complexity. All the methods before mentioned require a lot of time for evaluating data, changes in the setup and strong signals, which reduces the length range and the spatial resolution. Thus, in this paper, a technique for measuring dynamic variations of temperature or strain is proposed; it is based on the well-known anomaly detection method referred to as the RX-algorithm to process the data obtained by using a typical BOTDA system. This technique exploits the Brillouin sensing advantages without punishing complexity or performance limitations.

2. Theory

The stimulated Brillouin interaction in single mode fibers can be modeled by the three-wave transient equations among the pump (subscript p), the Stokes (subscript s) and the acoustic waves, with field amplitudes $E_{p,s}(z,t)$ and $E_a(z,t)$ in time t and position z along the fiber [13]. Brillouin sensors focus on measuring the backscattered light, which gives information about changes in temperature or strain in the fiber. Considering pump pulses larger than the phonon life time, no pump depletion and not negative intensity, the Brillouin backscattered light power $P_B(z,\nu)$ detected at the receiver can be given by:

$$P_s(z=0,\nu,t) = |E_s|^2 = \frac{c}{2n} g_B P(t) \exp(-2\alpha z), \quad g_B = \frac{g_0 (\Delta\nu_B/2)^2}{(\nu - \nu_B)^2 + (\Delta\nu_B/2)^2}, \quad (1)$$

where $P(t)$ is the total power of the launched pulsed light, α is the attenuation coefficient of the fiber, n is the refractive index, c is the velocity of light in vacuum and g_B is the Brillouin gain spectrum (BGS); in this case g_B has a Lorentzian shape and is assumed not to depend on z . The parameter ν_B is the frequency at which g_B has a peak value g_0 , and $\Delta\nu_B$ is the full width at half-maximum (FWHM). The Brillouin frequency shift (BFS) has a linear dependence on the applied strain ϵ and the temperature variation ΔT (at reference values of temperature T_0 and strain ϵ_0) [7,13]. Also, it is important to remark that there is an exponential relationship between the Brillouin power gain and the BGS, which is maximized at ν_B .

In BOTDA sensors, an optical pulse is launched in the fiber, and the backscattered light is detected by using an optical coherent detection method [14]. The backscatter power is recorded as a function of time. Providing that the velocity of light in the fiber is known, a time to distance conversion can be computed and a precise localization is possible. The width of the optical pulse can define the spatial resolution of the measurement, while the information collected at a given moment corresponds to the interaction that takes place on a position of the fiber; this position is defined by the length of fiber that was illuminated by the pulsed light. Figure 1 shows the BOTDA technique based on the successive recording of the Brillouin interaction at different specific frequencies. A complete frequency response of the fiber as a function of the distance is then compiled and the local BFS is computed by looking at the maximum of the Brillouin interaction at each location along the fiber.

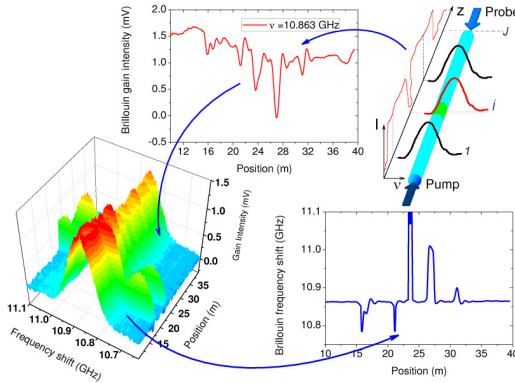


Fig. 1. Traces and fiber distribution of the Brillouin frequency shift.

The recorded distance of the fiber is divided in intervals that are defined by the length between two measurement points (Δz); thus the distance z is given by $J\Delta z$ (with J as the total number of points on the trace). Since the backscattered signal is weak, each trace of position versus Brillouin gain has to be obtained from an averaging process of N samples. A high value of N (~2000) improves the signal to noise ratio (SNR) of the data allowing a more accurate measurement. Each trace is obtained in a time interval Δt ($\Delta t \approx N\delta t$); hence the measurement time $T \approx M\Delta t$ can be defined by Δt and the number of frequencies evaluated M ($m = 1, 2, \dots, M$, being M the ratio between span and step frequency). Hence, the backscattered light power at each point j at frequency ν can be computed as:

$$\begin{aligned} \overline{\mathbf{P}}_s(\nu, t) &= \left(\overline{P}_{s1}(\nu, t), \dots, \overline{P}_{sj}(\nu, t), \dots, \overline{P}_{sJ}(\nu, t) \right), \\ \overline{P}_{sj}(\nu, t) &= \sum_{n=1}^N \frac{P_{sj}^n(\nu, t)}{N}, \end{aligned} \quad (2)$$

The maximum Brillouin gain along the fiber is constant under steady state conditions or slow variations of the medium that surrounds the whole fiber (hereafter named as natural Brillouin gain). Only with local and sudden variations of temperature (or strain) in the fiber, the Brillouin frequency distribution is locally displaced.

To reduce the measurement time, the N number could be decreased, but the accuracy on the measurement can be negatively affected. To overcome this lack, a special algorithm capable of detecting small events among the data (no matter how small the N number is) can be used, since dynamic events can be seen as temporally anomalies in the natural Brillouin gain. If the measurement is focused around the Brillouin peak gain, the required time is drastically reduced and dynamic events can be properly measured. Furthermore, it is possible to move the frequency of the probe according to a specific value, making only two or three measurements of frequency in a trace.

Dynamic events along a fiber can be detected by measuring the Brillouin gain variations in a random position or time (respect to the Natural Brillouin Frequency Shift, NBFS). This process can be considered similar to the process of detecting and identifying unknown targets in hyper-spectral imagery, which are widely used in pattern recognition schemes as object detectors [15]. Anomaly detectors can be considered as two-stage process: In the first stage, spectral anomalies or localized spectral differences are identified; in the second stage, the anomaly is identified as a target or a natural clutter. Anomaly detection algorithms attempt to locate anything that looks different spatially or spectrally from its surroundings, e.g. pixels that have a significantly different spectral signature from their neighboring background clutter pixels, or anomalies embedded within background clutter with a very low SNR.

In this paper, the RX-algorithm [15] is used as the method to detect dynamic events in distributed Brillouin sensors. This algorithm is a constant false-alarm rate (CFAR) anomaly detector that is derived from the generalized-likelihood ratio test (GLRT). In the RX-algorithm, anomaly detection is formulated as two hypotheses, H_0 and H_1 . The first hypothesis models the background as a Gaussian distribution with zero mean and an unknown background covariance matrix, which is estimated locally or globally from the data. The second hypothesis models the target as a linear combination of a target signature and background noise. So, under H_1 a spectral vector is represented by a Gaussian distribution with a mean equal to the signature of the target and a covariance matrix equal to the background covariance matrix in hypothesis H_0 . Let each signal data consisting of J points represented by the column vector $\mathbf{x}_i = \{x_{ij}\}_{j=1}^J$ with dimensionality I ; then, \mathbf{X} is an $I \times J$ data matrix. The two competing hypotheses for the RX-algorithm are given by:

$$H_0 : \mathbf{x} = \mathbf{j} \quad (\text{Target absent}), \quad H_1 : \mathbf{x} = a\mathbf{s} + \mathbf{j} \quad (\text{Target present}), \quad (3)$$

where $a = 0$ under H_0 and $a > 0$ under H_1 respectively. The vector \mathbf{j} represents the noise and \mathbf{s} is the spectral signature of the signal (target). The target signature \mathbf{s} and the background covariance C_i are assumed to be unknown. The model assumes that the data arise from two normal probability density functions with the same covariance matrix but different means. The background data H_0 is modeled as $J(0, C_i)$ and the data with the target present H_1 is modeled as $J(\mathbf{s}, C_i)$. In general, the hypothesis H_1 would have different covariance structure from H_0 , which should include the covariance of target magnitude. However, since the statistical structure of the anomaly a cannot be defined in the RX-algorithm, the same covariance matrix for anomaly and background is adopted. Then the RX-algorithm can be written as:

$$RX(\mathbf{x}_i) = (\mathbf{x}_i - \hat{\mu}_i)^T C_i^{-1} (\mathbf{x}_i - \hat{\mu}_i), \quad (4)$$

where

$$\hat{\mu}_i = \left(\frac{1}{J} \sum_{j=1}^J x_{ij} \right) \cdot \mathbf{1}^T, \quad \text{and} \quad C_i = \frac{1}{J} (\mathbf{x}_i - \hat{\mu}_i) \cdot (\mathbf{x}_i - \hat{\mu}_i)^T. \quad (5)$$

The here exposed dynamic detection technique for distributed Brillouin sensing uses I traces of dimensionality M ($i = 1 \dots I$; $m = 1 \dots M$) of the backscattered light power at the Brillouin frequency peak (M is the number of evaluated frequencies around the peak value);

the data are obtained each time interval Δt (time spent for measuring a trace). Since the RX-algorithm can detect variation from the clutter Brillouin data, the number N in this technique can be decreased in relation to the N used in traditional BOTDA systems. Hence, the power Brillouin gain on the fiber for I traces can be written by $\overline{\mathbf{P}}_s^m(\nu_B) = \overline{P}_{s\,ij}^m(\nu_B)$ ($\overline{\mathbf{P}}_s^m$ is an $I \times J$ matrix). In the case of using only the Brillouin frequency peak $M = m = I$ and $\nu = \nu_B$.

Therefore, spatially detection of anomalies along the fiber, and detection of anomalies on the fiber along the time can be located or determined by adapting Eq. (4) and Eq. (5) to data of power Brillouin gain as function of position (\mathbf{RX}_p) or time (\mathbf{RX}_t) by:

$$\mathbf{RX}_{Y\,j}^m \left(\overline{P}_{s\,ij}^m \right) = \left(\overline{P}_{s\,ij}^m - \mu_{Y_{ij}}^m \right)^T C_{Y_j}^{-1} \left(\overline{P}_{s\,ij}^m - \mu_{Y_{ij}}^m \right) \quad Y \equiv p \text{ or } t, \quad (6)$$

with

$$\begin{aligned} \hat{\mu}_{p_j}^m &= \mu_{p_{ij}}^m = \left(\frac{1}{I} \sum_{i=1}^I \overline{P}_{s\,ij}^m \right) \cdot \mathbf{1}^T; \quad C_{p_j} = \frac{1}{I} \left(\overline{\mathbf{P}}_{s\,j}^m - \hat{\mu}_{p_j}^m \right) \cdot \left(\overline{\mathbf{P}}_{s\,j}^m - \hat{\mu}_{p_j}^m \right)^T, \\ \hat{\mu}_{t_i}^m &= \mu_{t_{ij}}^m = \left(\frac{1}{J} \sum_{j=1}^J \overline{P}_{s\,ij}^m \right) \cdot \mathbf{1}^T; \quad C_{t_i} = \frac{1}{J} \left(\overline{\mathbf{P}}_{s\,i}^m - \hat{\mu}_{t_i}^m \right) \cdot \left(\overline{\mathbf{P}}_{s\,i}^m - \hat{\mu}_{t_i}^m \right)^T. \end{aligned} \quad (7)$$

The $\mathbf{RX}_{t\,i}^m$ and $\mathbf{RX}_{p\,j}^m$ components can be obtained from the data of a conventional BOTDA system, without any change on the setup, only using the information that come out from the photoreceptor. The implementation of the RX-algorithm can be made on the processing or post-processing stage. These components show information about dynamic events on time and the position on which they emerge on fiber for a given Brillouin scattering condition.

3. Experimental results

To experimentally demonstrate the feasibility of using anomaly detectors, in particular the RX-algorithm in standard BOTDA systems, three main concepts are carried out. First, the capability of detecting and isolating dynamic events from static events; second the influence of N number in the dynamic detection; and finally, detection of multiple spatial events along the fiber and detection of multiple events on time.

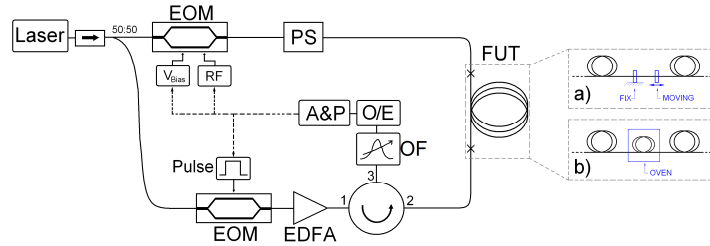


Fig. 2. Experimental setup. Strain a) and temperature b) configuration. PS is the polarization scrambler, FUT is the fiber under test, V_{Bias} is the bias voltage, RF is the RF generator, OF is the optical filter, O/E is the photodiode, and A&P is the analysis and processing unit.

The BOTDA setup used is depicted in Fig. 2. Pump and probe signals are obtained from the same laser source (at 1550 nm) by using a Mach-Zehnder electro optic modulator (EOM), as well as the optical pulses that have a sampling rate of 2 KHz. The time-domain signals are monitored with a high speed photodiode. This BOTDA system uses 5 ns and 10 ns of pump pulse at 120 mW and 0.1 m of sampling interval. A segment of the optical fiber is dynamically strained using a step motor and its temperature is varied by using a resistive oven (inset figures in Fig. 2).

The first step of the proposed technique requires a preliminary frequency scan process to measure the BFS along the fiber and determine the NBFS. Once the BGS is obtained, the dimensionality M has to be defined. For simplicity, the value M is set to 1, i.e. $\nu = \nu_B$. So, in

this case the event detection is focused on the exponential decaying behavior of the Brillouin gain around its maximum. Figure 3 shows the results of RX-algorithm at $\nu = \nu_B$ for a fiber section linearly strained that is placed at 2783.8 m, and the BGS of the same section without strain and a pumped light of 10ns (line dot in Fig. 3).

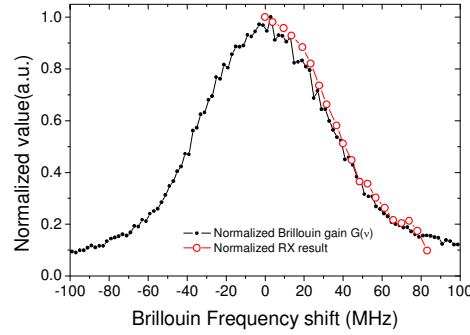


Fig. 3. Exponential decaying behavior of the BGS around ν_B for strain variations on the fiber.

To prove the capability of the technique for distinguishing between dynamic and static events, two sections of 0.5 m and 1 m are statically strained (1 and 2 in Fig. 4), while other two of 1 m are strained only for 100 seconds (3 and 4 in Fig. 4). Fiber sections 1 and 2 are compressed 1500 $\mu\epsilon$ and strained 4000 $\mu\epsilon$ respectively, and sections 3 and 4 are dynamically strained 2800 $\mu\epsilon$ and 800 $\mu\epsilon$ respectively. In these measurements, the BOTDA system uses 5 ns, N is equal to 1000 and Δt is 4 seconds. By making a simple skimming of Fig. 4.a, the only highlighted section from data is the third one, as well as the temporally behavior of this section. The classical measurements of BFS are obtained by completing a frequency swept. If the swept has a span of 360 MHz and step of 1 MHz, it takes 7.6 minutes (including the time spent by the electrical system and the acquisition card). Hence, the strain events have to take at least 430 seconds ($T = 430$ s).

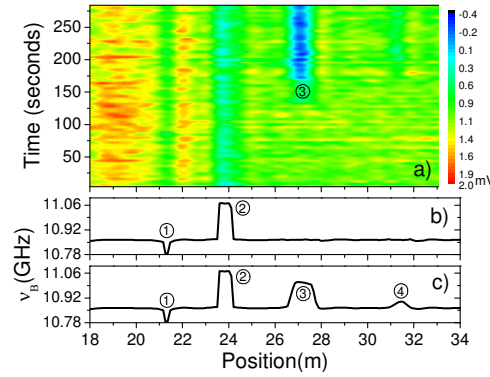


Fig. 4. a) Brillouin intensity at $\nu_B = 10.86$ GHz with no further analysis, i.e. $\overline{P}_{s\,ij}^m(\nu_B)$ with $m = 1$. b) BFS obtained by traditional BOTDA swept for the two static and the two dynamics fiber sections. c) All the fiber sections are statically strained at the values of used in Fig. 4.a.

In order to have a reference technique, a direct measurement of the minimum intensity at ν_B [8] (because the system is in Stokes gain regime) is used to compare with. It consists on measuring the minimum value at each position point from the vector $(\overline{P}_{s\,1j}^m(\nu_B), \dots, \overline{P}_{s\,ij}^m(\nu_B), \dots, \overline{P}_{s\,iJ}^m(\nu_B))$ or time in vector $(\overline{P}_{s\,i1}^m(\nu_B), \dots, \overline{P}_{s\,ij}^m(\nu_B), \dots, \overline{P}_{s\,iJ}^m(\nu_B))$. The result of this reference technique (hereafter denoted as minimum) on data of Fig. 4.a is shown as the dash-dot line in Fig. 5.a. From this figure two facts can be remarked; first, the static and dynamic events on sections are exposed as minimum peaks; and second, there is not a clear a

base noise to efficiently set a threshold event. As part of the dynamic technique, the RX-algorithm is applied to the same data of Fig. 4.a; results are depicted as the continuous line (blue) in Fig. 5.a. An important issue is revealed at first sight: the static events are suppressed while the dynamic events remain clear; also the noise base is constant and less noisy, being optimum for an efficient setting of a threshold.

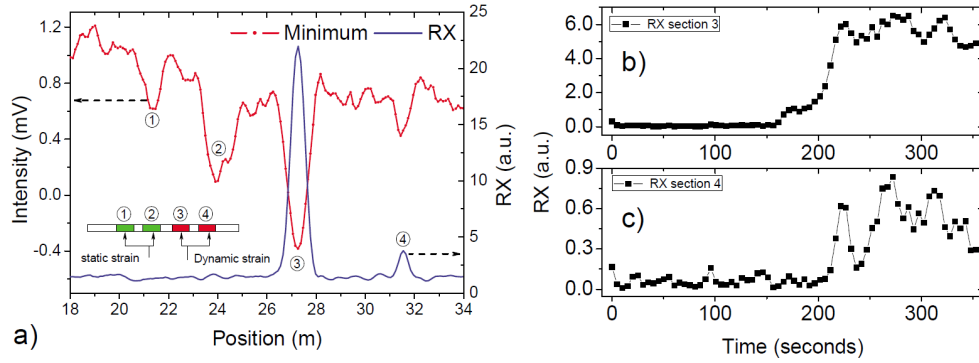


Fig. 5. a) Dynamic detection. Strain evolution on time of b) Section 3 and c) Section 4.

After exposing the capability for detecting dynamic events, the minimum value of N to obtain reliable results using RX-algorithm is investigated. If N is large, the noise of the measured trace can be reduced, but the time interval Δt is increased; N also depends on the spatial resolution and the measurement distance, i.e. the Stokes signal coming from a larger distance of 8 Km is weaker than a Stokes that comes from hundred meters of distance on the same fiber. To better explain the above idea, an optical fiber of 3000 m, a section of 1 m is stressed twice by a step motor 800 $\mu\epsilon$ during 20 s each 40 s. Results are summarized in Fig. 6.

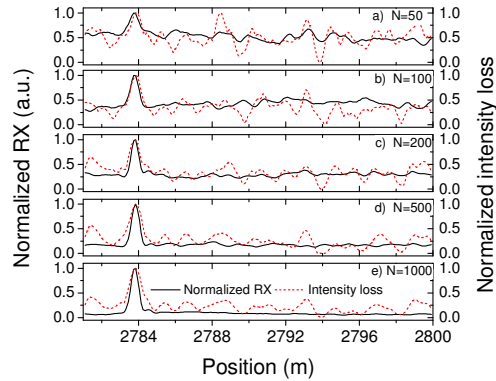


Fig. 6. Comparison between minimum and RX-algorithm techniques for different values of N .

Figure 6 shows normalized RX-algorithm results (continuous line) and normalized minimum intensity losses (dashed line) for 5 values of N . The evolution of segment in the fiber is cleaned up and the dynamic event is highlighted from the clutter Brillouin intensity. This is a measurement on how this dynamic event can be spatially detected, maintaining constant the event duration and the strain value. It shows a SNR >10 dB for $N = 200$, significant if it is considered that Δt is reduced from 6.83 s at $N = 1000$ to 4.26 s at $N = 200$.

Detection of multiple dynamic events is depicted in Fig. 7. The first part shows measurement of one to four events at different values of strain using $N = 1000$. In Fig. 7.a and 7.e the fiber section is strained 1500 $\mu\epsilon$, in Fig. 7.b and 7.f the sections are strained 1200 $\mu\epsilon$ and 1500 $\mu\epsilon$, in Fig. 7.c and 7.g the sections are strained 1200 $\mu\epsilon$, 225 $\mu\epsilon$ and 1500 $\mu\epsilon$, and in Fig. 7.d and 7.h the sections are strained 1500 $\mu\epsilon$, 900 $\mu\epsilon$, 300 and 500 $\mu\epsilon$. In the second part of the figure (Fig. 7.e to h) the detection of the defects is made with $N = 200$ and compared to

the minimum intensity losses. Figure 8 shows that the technique can also be used for measuring one dynamic event, which has different values of duration on time (Fig. 8.a) and when it is periodic along the time (Fig. 8.b).

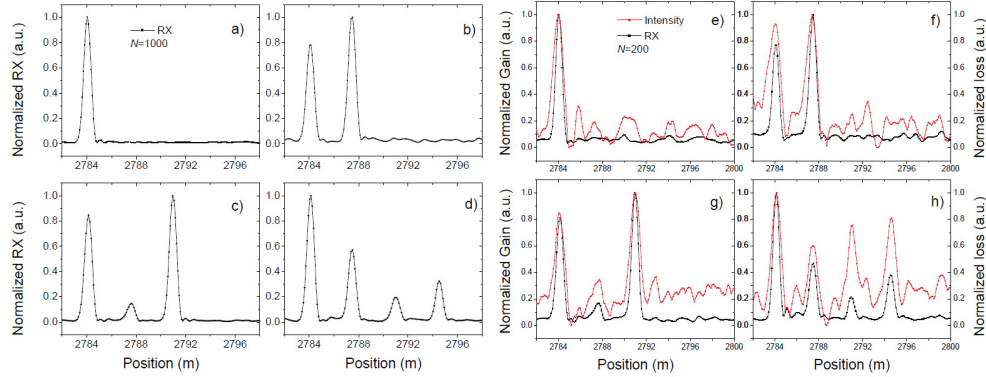


Fig. 7. Detection of multiple spatial events by using RX-algorithm.

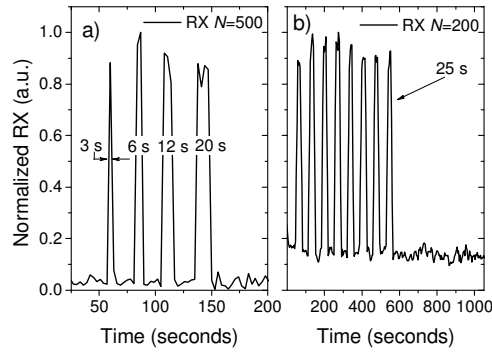


Fig. 8. a) RX-algorithm analysis of 1 m fiber section placed at 1078.5 m and strained $740 \mu\epsilon$ for events with duration of 3, 6 12 and 20 seconds and b) for 8 events of 25 seconds. The capture time between each trace is 3 seconds.

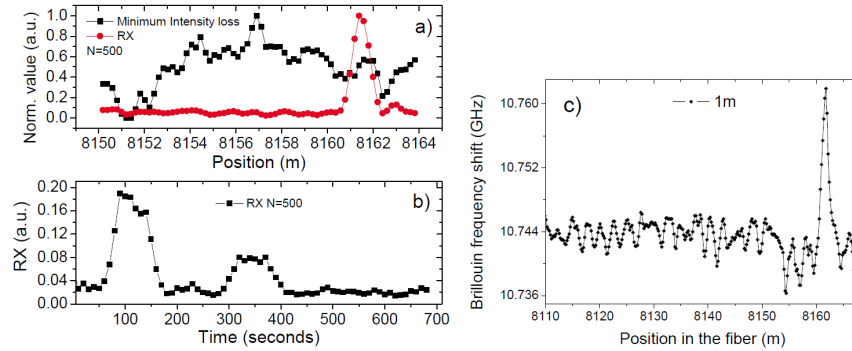


Fig. 9. a) RX-algorithm analysis for fiber section of 1.2 m strained $1500 \mu\epsilon$ and $860 \mu\epsilon$. b) Events occur during 90 seconds separated 2 minutes. c) BFS obtained by sweeping the probe for a span of 170 MHz and a step of 1 MHz, when the segment is statically strained $860 \mu\epsilon$.

Figure 9 shows event detection on a fiber section of 1.2 m stressed twice at 8000 m. A complete measurement of BFS takes ~ 6 minutes, which is not enough time for registering the events, while data in Fig. 9.b is taken each 10 seconds. Additionally, it is important to remark

that the minimum intensity measurement does not distinguish spatially the strain even at v_B , whereas it is highlighted by using the RX-algorithm.

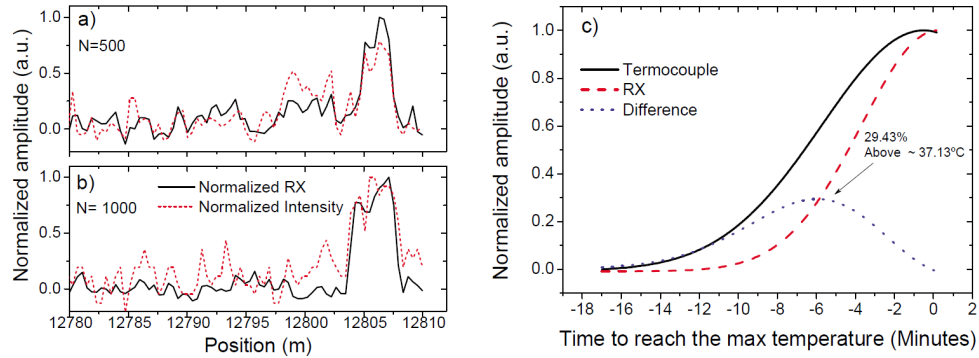


Fig. 10. Measurement of temperature by using RX-algorithm analysis. The BOTDA system uses a pump pulse of 25 ns, a sampling interval of 0.4 m and a Δt of 6.06 s. The section measured is the same in both cases under the same conditions.

The technique exposed in this paper is also validated for measuring temperature changes. Figure 10 shows the detection of a dynamic event corresponding to a fiber section of 4 m placed into an oven located at 12.8 Km from the origin (Fig. 10.a). The temperature inside the oven is measured by using a thermocouple, which varies with an exponentially shape from 22.7 °C to 75.6 °C as it is shown in Fig. 10.c. The data analyzed with the dynamic technique exposes the fiber segment affected by the temperature; it also shows that the temperature in the section follows the same tendency and shape that the data obtained with the thermocouple. However, the technique starts measuring the temperature variation after 37 °C, i.e. the temperature threshold is placed 14.3 °C above the initial temperature.

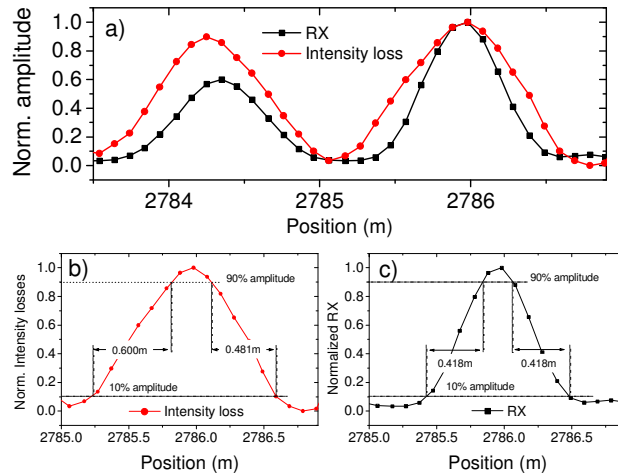


Fig. 11. a) Two fiber sections of 0.5 m spaced 0.5 m and strained 1220 $\mu\epsilon$ and 1460 $\mu\epsilon$. The BOTDA system uses a pump pulse of 5 ns, a spatial interval of 0.1 m and $N = 500$. Calculation of spatial resolution using the rise and the fall time for b) Intensity losses and c) RX-algorithm.

Finally, it can be remarked that by using the proposed technique, the spatial resolution can be slightly improved. This fact is illustrated in Fig. 11 for data of Fig. 7. A spatial resolution of 0.418 m is measured using the RX-algorithm in the technique, whilst a spatial resolution of 0.541 m is measured by using the minimum.

4. Discussion and Conclusions

Detection of dynamic events by BFS implies that the sensor system satisfies the criterion of the sampling theorem, i.e. the sensor has to provide a sampling rate at least half the duration of the event. By using anomaly detection method, this rate can be reduced one order of magnitude; such is the case of Fig. 4 with m equal to 360 (span of 360 MHz and step of 1 MHz) for a conventional BOTDA, while in the anomaly detection method presented in Fig. 5, m is equal to 1. In the first case a complete measurement takes ~ 7 minutes, which implies that events faster than 430 s are not fully detected. Then the dimensionality on $\overline{\mathbf{P}}_s^m(\nu_B)$ establishes a span-step-frequency ratio related to T and with the sampling rate. In the proposed technique it is not necessary to use only the frequency ν_B , neither the whole frequency span, instead as an alternative a discrete frequency span can be used. The number of averages was analyzed to describe its influence on the quality of the measurements, this quality can be characterized by the SNR, and the experimental results suggest that in 3 Km only 200 averaging is needed to obtain a clear discrimination of dynamic events. This conclusion can also be extended to detection of two, three or four defects in the same spatial interval. Additionally, it was proved that this technique allows a good dynamic detection for ranges of 8 Km and 12.8 Km with defects of 1.2 m and 4 m length respectively, which can be used to measure and detect temperature or strain variations. And lastly but not less important, it was found that the spatial resolution for a pump pulse of 5 ns can be enhanced up to 0.418 m, since the analysis is concentrated in the variation of the Brillouin gain value and not only on the averaging value of the signal along the time.

To conclude, a technique for measuring dynamic variations of temperature or strain, which is based on a standard BOTDA system, anomaly detection methods and Brillouin gain spectrum, is proposed. This technique provides dynamic sensing at a randomly addressed position at a sampling rate only limited by the time-of-flight of the pulses and the acquisition card. A simple proof-of-concept has been performed to demonstrate the capabilities of this technique, using a RX-algorithm and the exponential decaying behavior of the Brillouin gain around its maximum. The RX-algorithm provides information on how a dynamic event differs from its static state. Additionally, the dynamic technique reported in this paper clearly detects variations on the temperature and the strain in a fiber section. Furthermore, the spatial resolution with the technique based on the Stokes gain regime can be improved, since the analysis is concentrated in variation of the Brillouin gain and not only on the averaging of the signal.

Finally, it must be mentioned that the BOTDA system is standard and it does not experience any alteration on its setup or detriment on the signal, neither it is punished with a complex analysis implementation, which can be costly for measuring dynamic events.

Acknowledgments

The authors acknowledge the financial support from the Spanish Ministry of Education through the project TEC2010-20224-C02-02.